Table des matières

I. Introduction 2
A. Medical context 6
1. Prostate tumours 7
2. Eye plaque treatment 17
B. Physical context 26
1. Dosimetry 26
2. Microdosimetry 36
II. Theoretical background: definitions and protocols 42
A. Dosimetric quantities 42
1. Fluence and Energy Fluence 42
2. Kerma 43
3. Absorbed dose 44
B. Microdosimetric quantities 45
1. Linear Energy Transfer: LET 45
2. Energy deposit εi 45
3. Energy imparted ε 45
4. Specific energy z 45
5. Lineal energy y 46
6. Microdosimetric spectra 47
C. Dose Formalism for radioactive seeds : TG-43 47
1. Dose rate constant, Λ 48
2. Geometry factor, G(r,θ) 48
3. Radial dose function, g(r) 49
4. Anisotropy function, F(r,θ) 49
D. Nederlandse Commissie voor Stralingdosimetrie (NCS) protocol for external photon beam dosimetry 50
III. Dosimetry
54
A. Material 54
1. Monte Carlo simulation 55
2. Measurements 66
B. Method 72
1. Monte Carlo simulations 72
2. Measurements 82
C. Dosimetric results 90
1. Dosimetric data 91
"Dosimetric study of the new InterSource125 iodine seed" 94
"Dosimetric study of a new palladium seed" 101
"The radial function of low energy Brachytherapy seeds in different solid phantoms: comparison between calculations with the EGSnrc and MCNP4C Monte Carlo codes and measurements." 115
2. Water equivalence 130

IV. Microdosimetry 138
A. Introduction 138
1. The microdosimetric approach 138
2. The ionization cluster approach 143
"Theoretical analysis of Microdosimetric spectra and cluster formation for 103Pd and 125I photon emitters" 145
V. Conclusion 162

I. Introduction

The word *brachytherapy* is derived from the Greek word "brachios" meaning short and refers to the therapeutic use of encapsulated radionuclides within or close to a tumour. The history of brachytherapy is nearly as old as the history of radioactivity itself. Already in 1901, Pierre Curie suggested to Dr A. Danlos at St. Louis Hospital in Paris that a small radium tube be inserted into a tumour thus heralding the birth of brachytherapy. In 1903, Alexander Graham Bell made a similar suggestion, completely independently, in a letter to the Editor of Archives Roentgen Ray. It was found in these early experiences that inserting radioactive materials into tumours revealed that radiation caused cancers to shrink. In 1913, so only 17 years after Becquerel discovered natural radioactivity, one of the two totally new pavilions opened with the assistance of the Pasteur Institute and the University of Paris under the name “Institut du Radium” to study radioactivity was dedicated to medical and biological research. Radium therapy was developed just after the First World War, around 1920. The Manchester system for implantation of radium needles was introduced as early as 1934, the same year as artificial radioactivity was discovered.

World War II halted all the medical nuclear research and the first attempt to introduce new sources in the United States were by William Myers and Ulrich Henschke. Myers introduced for clinical use in 1948 sources of ^{198}Au, ^{60}Co, ^{32}P and also one of the isotopes that concerns us, ^{125}I and Henschke standardised an afterloading system utilising plastic tubes and ^{198}Au seeds in 1953. Later on, Henschke and Basil Hilaris developed a school based on the afterloading technique with ^{137}Cs and ^{192}Ir particularly for cervix and other deep seated carcinomas.

These new isotopes, being less energetic than Radium, allowed a more precise positioning of the sources while keeping the dose to the fingers of the operator to an acceptable level. Major developments of the new methods with ^{137}Cs and ^{192}Ir occurred after 1955 at the Gustave –Roussy Institute with Bernard Pierquin, Daniel Chassagne and Andrée Dutreix. During 1965 and 1966, Pierquin and Dutreix have determined the rules for a new implantation system which they named the Paris System. (Bartelink et al. 1988).

Brachytherapy also represents one of the oldest techniques of radiation therapy for prostate cancer. In 1911 Pasteau (Pasteau 1911) published the first report on brachytherapy treatment for prostate cancer, which involved the simple insertion of radium into the prostatic urethra via a catheter. In 1922 Denning published a series of 100 cases treated by this technique (Denning 1922). Although short-term local control of the disease was surprisingly good for this crude method, the complications were significant, occurring in about 15 to 20 percent of patients. In 1972 an open-

surgical, retropubic brachytherapy method with permanent implants used for the radiation source was introduced by Whitmore et al (Whitmore et al. 1972) at Memorial Sloan-Kettering using ^{125}I and by Carlton et al (Carlton et al. 1972) using ^{198}Au in combination with external-beam radiation therapy.

Even if in the beginning the positioning of the seeds for the prostate implants was far from accurate, the technique has been improved greatly through the years thanks to, for example, the introduction of image guided implantation methods. Software incorporated in commercial ultrasound units were developed that accurately display the template coordinates superimposed over real-time images of the prostate, providing targets for the accurate placement of needles into the prostate. These developments appear to have overcome many of the inaccuracies inherent with the open-surgical, retropubic method of seed insertion. Three-dimensional dose distributions are calculated for the prostate, rectum, and bladder, and variables can be adjusted to optimize the dose to the prostate and minimize the dose to adjacent tissues. This method facilitates the creation of an idealized implant, customized to account for the wide range of individual prostate sizes and shapes.

Most experience with brachytherapy for prostate cancer involves the use of ^{125}I as a permanent implant. ^{125}I emits low energy photons (27 keV) and has a half-life of 60 days. The advantage of low energy is the ease of radioprotection for medical workers and the confined volume of radiation dose from the implant that minimizes the dose to surrounding healthy tissues. As will be emphasized in this work, at this energy level, tissue absorption becomes an important factor. Meticulous attention must be given to the accurate placement of ^{125}I sources. Otherwise dose inhomogeneities within the implant area may easily occur, leading to areas of underdosage and tumour sparing. The relatively long half-life results in an initial peripheral dose rate of 7 cGy/hr when a total dose of 144 Gy is prescribed. This low dose rate has raised concerns about the effectiveness of ^{125}I for rapidly dividing malignancies. Laboratory experiments have demonstrated that in rapidly dividing tumours proliferation may occur during the course of an iodine implant, potentially reducing the degree of cell kill (Ling 1922, Freeman et al. 1982).

As a reply to this concern, ^{103}Pd was introduced in 1986 as a new, permanently implantable radioisotope for use in brachytherapy. The physical dimensions of ^{103}Pd seeds have been chosen to be identical to those of ^{125}I, and therefore implantation devices designed for^{125}I can be used for ^{103}Pd as well. Its photon energy is close to ^{125}I at 21 keV, but its shorter half-life (17 days) yields a higher initial dose rate of about 20 cGy/hr as compared with 7 cGy/hr obtained with ^{125}I. Because of its low energy, ^{103}Pd demonstrates advantages of radioprotection and confined dose and the rapid decrease in dose similar to the characteristics of ^{125}I. Although the amount of clinical data reported for this new source is still smaller than for ^{125}I, it is hoped that the higher dose rate will address some of the radiobiological concerns raised

by the low dose rate of ^{125}I and will result in the successful treatment of poorly differentiated malignancies.

Radiation therapy has also been proposed in the beginning of the 1930s as an alternative to enucleation in the case of choroidal melanoma as a way to save the eye and to some extent, vision. Since then, several isotopes have been tested including ^{103}Pd and ^{125}I. The low energy of these two isotopes makes them the ideal choice to spare as much as possible the healthy tissues surrounding the tumour, which in this case are mainly the lens and the optical nerve. For this application too, treatment planning systems (TPS) have now been developed that permit to calculate very accurately the dose distribution inside the eye and to optimise the treatment according to the position of the lesion relative to the tissues at risk.

It is clear that we have come a very long way since Pierre Curie proposed the idea that perhaps radiation could be used to treat cancers. With the diversity of the available sources, the improvement of the techniques to increase the precision of the positioning and the development of computers and software that allow calculating very quickly and precisely the dose distribution around the sources, it is presently possible to deliver the dose to the tumour quite accurately.

However, some questions remain open, especially for the low energy photon emitters. Indeed, even if ^{125}I was introduced quite early, its use was much less common than isotopes of higher photon energies like ^{192}Ir or ^{137}Cs until a few years ago. This is without even speaking about the huge amount of expertise acquired using external radiotherapy with ^{60}Co or megavoltage beams from linear accelerators. The advantages of the use of these low energy photons have been obscured for a long time by the fact that the positioning accuracy was very poor, which was responsible for large side effects. Now that this deficiency is partially solved, their natural advantages of radioprotection for the staff and of sparing of organs at risk are again predominating. A lot of work has then been done these last few years to bring the knowledge on low energy photon isotopes at a higher level. This includes, for the physical side, improvement of the primary standard for the calibration of the activity, a formalism to assess the dose distribution around the seeds, improvement of the calculations of the dose distributions or tests to find better methods of measurements in the low dose rates and high gradients around the sources. It is in this context that the first part of this work is situated.

Another open question concerns the biological effectiveness of these low energy photons. If the Relative Biological Effectiveness (RBE) of ^{192}Ir or ^{137}Cs are quite well known, it is not the same for photons around 20 or 30 keV. The ionizations produced when these photons traverse matter are spread more densely than for higher energy photons. A higher ionization density is known to be related to a higher efficiency to create damage to the cells in living tissues as it is more damaging for the DNA. In the second part of this work, we have investigated the problem of the spatial pattern of the

ionizations produced with ^{125}I and ^{103}Pd in nanometric volumes, chosen to simulate portion of the DNA, and the energy deposition at a microscopic scale.

A. <u>Medical context (Washington and Leaver 2004, NICER , COMS website)</u>

Iodine-125 can be used both in temporary or permanent implants. The type of temporary implant that will be used as an example in this work, because it is the more common, is eye plaque treatment. For the placement of a radioactive plaque, the patient usually is admitted to the hospital. An incision is made in the conjunctiva, a thin membrane which covers the outside of the eye (see box 3, page 18), and the radioactive plaque is stitched to the outside of the eye over the tumour (see Figure 1a). The conjunctiva is then sewn back over the plaque. After approximately three to seven days, surgery is performed again to remove the plaque.

The main example for permanent implant is the treatment of prostate cancers. Permanent implants are performed when the tumour to be treated is difficultly accessible making the removal of the radioisotope impossible or impractical. ^{125}I, ^{103}Pd or also ^{198}Au are ideally suited for permanent implants because of their short half-lives. The patients who receive these types of implants do not have to undergo a second surgical procedure to remove the isotopes. The volume to be treated requires the placement of many sources; this requires rapid and accurate methods of application. To accomplish this, gun type applicators with a long, hollow insertion needle are often used. Often, computer tomography (CT) guided, the needle is pushed through the skin into the deep tumour, and the sources are inserted into the tumour (see figure 1b). The needle is then withdrawn 5 to 10 mm and the next source is inserted. This is repeated until the desired length and the desired number of sources are applied. Permanent implants using ^{125}I, ^{103}Pd or ^{198}Au are ideally suited for deep-seated lesions in the pelvis, abdomen and lung.

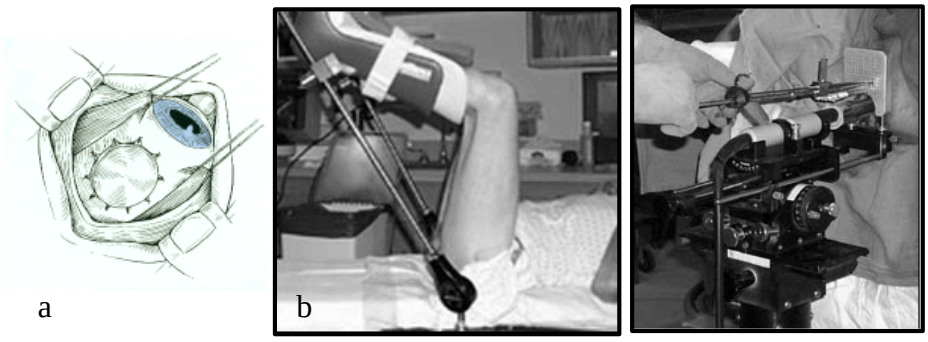

Figure 1: Methods of source implantation for eye treatment and prostate.

In the following paragraphs we will briefly describe the two most common sites that are treated with low energy isotopes: prostate and eye.

1. Prostate tumours

Prostate cancer is a malignant growth originating in the cells of the prostate gland (see box 1 for anatomy description) and is therefore described as adenocarcinoma (or glandular cancer). Carcinoma of the prostate is one of the most common malignancies in males in the US, where approximately 1 man in 11 develops prostate cancer. 80% of this carcinoma occurs in men over 65 years old. Strong prognostic indicators are the clinical stage and pathologic grade of tumour differentiation* (see box 2). Larger and less differentiated tumours are more aggressive and have a greater incidence of lymphatic and distant metastases.

a) Treatment techniques

The management of these tumours has several areas of controversy. The natural history of this tumour is variable and influenced by multiple prognostic factors and the different possible treatments can affect the quality of life and sexual function to varying degrees. The different treatments proposed are:

(1) Observation:

For patients older than 75 years, observation is reasonable management. It can be proposed too for younger patients when the tumour is small and well-differentiated. For many urologists a T1a (see box 2) disease found incidentally requires no treatment as many years will pass before it becomes a clinical problem. Moreover, only 6.8% of the patients at that stage show a progression in their disease.

(2) Prostatectomy:

Patients with resectable stage T1 and T2 prostate tumour who are in good general medical condition and have a life expectancy of at least 10 years are candidates for radical prostatectomy. In classical prostatectomy, close to 100% of the patient suffered of impotency after the surgery. Nowadays, nerve sparing surgery is privileged, so a lower incidence (40 to 60%) of sexual impotence has been reported. Radiation therapy has been shown to provide very similar results. For good prognosis patient (PSA† ≤ 10 ng/ml, Gleason‡ ≤ 6), 78% of irradiated patient and 80% of the

* Whether or not the cancer is likely to grow slowly or very quickly depends on how closely the cells of the cancer resemble normal cells. Those that appear very much like normal glandular tissue with some cancer cells in the lining are termed well differentiated cancers. Those that appear very little like normal glands and more like sheets of packed cancer cells are termed poorly differentiated cancers. Those which form multiple small glandular spaces are in the middle and are called moderately well differentiated cancers.

† Prostate-Specific Antigen

‡ More detailed descriptions of the cancers have been given by pathologists and describe the tissue in terms of Gleason grade.

prostatectomy patient were disease-free 5 years after treatment by PSA criteria.

(3) Hormonal therapy:

A regression of the tumour has been shown after orchidectomy (removal of the testicles) or estrogen administration. Hormonal therapies seek to reduce the androgenic stimulation of prostatic carcinoma.

- Well differentiated cancers have a low Gleason grade (grade 2-4).
- Moderately well differentiated cancers have a moderate Gleason grade of 5 or 6.
- Poorly differentiated cancers have Gleason grades 8, 9, or 10

Well differentiated cancers tend to grow slowly and take a long time to become clinically significant. Their doubling time or the time it takes for the tumour to double in size is measured in terms of years. Moderately well differentiated cancers with a Gleason grade of 5 or 6 may become clinically significant if they occur in younger men below the age of 70-75. Over the age of 80, the patient is more likely to die of other causes than his prostate cancer. Poorly differentiated cancers are described as Gleason grades 8, 9, or 10 and these tumours are very aggressive, have poor results with most treatments, and have doubling times which are measured in a matter of weeks or months. Grade 7 cancers act in between the moderate and high grade cancers and must be considered significant, but not incurable cancers.

Box 1: Anatomy of the prostate

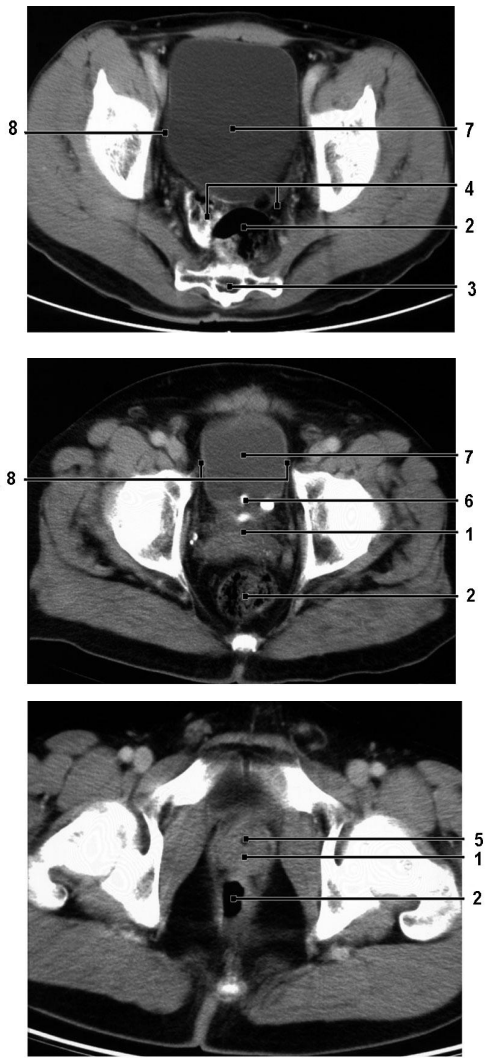

1. prostate
2. Rectum
3. Sacrum
4. Seminal vesicle
5. Urethra, male
6. Urethra, prostatic
7. Urinary bladder
8. Urinary bladder, detrusor

(4) Chemotherapy:

Several drugs have been tested in patients where the hormone therapy has failed. It is beyond the scope of this work to detail all the possible chemotherapy drugs.

(5) Radiotherapy:

(a) External radiotherapy

For patients with a stage T3 disease most urologists and radio-oncologists agree that radiotherapy is the treatment of choice, usually combined with hormonal therapy. Because of significant tumour bulk and high metastatic potential of this category of disease, radiation alone was not satisfactory, with only 10% to 35% PSA disease-free survival at 10 years. The addition of hormone therapy has largely improved that result to 78% versus 33% at 6 years.

The volume to irradiate must first be agreed on, with or without the seminal vesicles. In general, because treating the seminal vesicles involves irradiation of a larger volume of the rectum, this concerns only patients with a PSA greater than 10 ng/ml and tumours with Gleason score greater than 6. It is also controversial if the pelvic lymph nodes must be irradiated. Different irradiation schemes are possible. The simpler is the classic technical box, with 4 fields, one anterior, one posterior and two lateral, with additional shielding. More sophisticated techniques exist as conformal three dimensional treatments. These techniques involve sophisticated radiation TPS and 3D CT reconstruction of the volume to be irradiated. Beam design may vary in this case. It is commonly a six fields configuration with blocks or Multi Leaf Collimator (MLC) to shape or conform each field. The typical doses are 50 Gy to the pelvic nodes, 54 to 56 Gy to the seminal vesicles if they are involved and 70 to 80 Gy to the prostate. Intensity Modulation Radiation Therapy (IMRT) is a more advanced technique which specifies the chosen dose to the tumour volume as well as acceptable dose levels for surrounding organs such as bladder, rectum and femoral heads. It involves 6 to 7 beam angulations with several different MLC settings in each field in order to create fluence modulation. This technique allows increasing the dose to the prostate while still sparing the organs at risk. Doses of 80 Gy or more can be delivered to the prostate using IMRT.

(b) High Dose Rate (HDR):

High dose rate ^{192}Ir is a way to deliver a boost following a moderate dose external beam treatment. Compared to ^{125}I and ^{103}Pd, which are permanent implants, this is a temporary implant technique. Similar to permanent isotopes, a perineal template is used to introduce needles and catheters into the prostate. The catheters are left in place and the patient is hospitalised. Total doses and fractionation are very variable from one trial to

another. Total doses and fraction sizes have varied as radiobiological dose equivalents of these large fractions are being established.

(c) Interstitial implants:

Radioisotopic implant is also an option for early stage (T1c, T2a-b), low grade (Gleason ≤ 6), low PSA (PSA ≤ 10ng/ml) prostate tumour. PSA-free survival appears very similar to external radiotherapy with 80% to 90%.

The proportion of patient treated by brachytherapy seeds is rapidly increasing because it offers several practical and theoretical advantages over external radiotherapy in selected patients. Firstly, the rapid fall-off of the dose in tissues allows dose escalation within the tumour while keeping the dose to the organs at risk reasonably low. Secondly, target motion, set-up variation and localization errors from day-to-day are not of major concern as they are with external treatment. It is estimated that about half of the patients diagnosed with prostate tumour will be treated with seed implants by 2006. (Nag et al. 1999)

Since late-1980's, the advent of transrectal ultrasound (TRUS) permits the use of a transperineal template technique. This procedure is done with either spinal or general anaesthesia and uses a grid or template against the perineum with the patient in the dorsal lithotomy position (see figure 1). Transrectal ultrasound is used to direct the needles, which are either preloaded, used with seeds in suture or with a Mick Applicator (see figure 2) that deposits the radioactive seeds. Dosimetry planning may be done in advance by taking ultrasound images every 5 mm from the base of the prostate through the apex and then loading these into the treatment planning computer. Seeds are then distributed throughout the prostate (see figure 3). Isodoses are computed (see Figure 4). Alternatively, this planning can be done in the operation room just before the procedure. In general, for the average gland, approximately 25 needles and

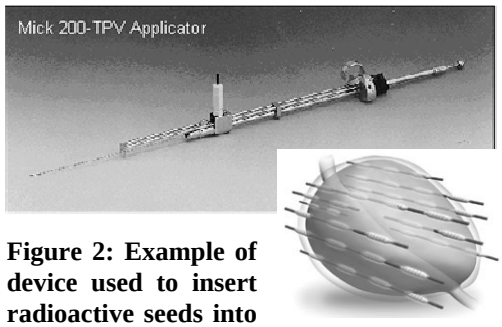

Figure 2: Example of device used to insert radioactive seeds into the prostate

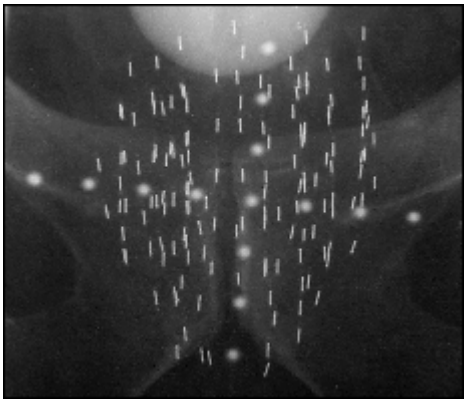

Figure 3: CT-scan image of a prostate implant with radioactive seeds

100 or so seeds are used. The current used permanent isotopes are ^{125}I and ^{103}Pd. The prescription dose recommended by the American Brachytherapy Society (ABS) and by the European Society for Therapeutic Radiology and Oncology (ESTRO) for implant alone with iodine is 145 Gy and with palladium is between 115 and 120 Gy. The prescribed dose is defined as the minimum peripheral dose to the margin of the target volume.

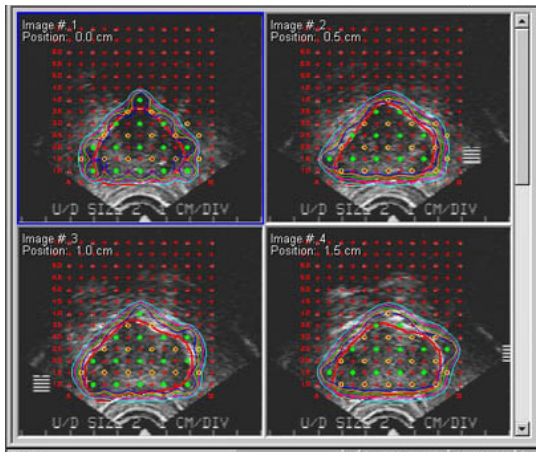

Figure 4: Example of TPS display to calculate the dose distribution calculated for a prostate implant based on TRUS

Organisations like ABS in 1999 in US (Nag et al. 1999) or ESTRO (ESTRO/EAU/EORTC) in 2000 (Ash et al. 2000) in Europe have made specific recommendations for the transperineal permanent brachytherapy of prostate cancer. Both recommend first that the patients are carefully selected. Only patients with a life expectancy greater than 5 years should be implanted. These patients must also be able to endure the surgical procedure and should not suffer of distant metastasis. They recommend also to evaluate carefully patients who have undergone transurethral resection of prostate (TURP) as there is a risk of seed loss and a higher risk of incontinence. Both groups give a maximum volume for the prostate beyond which they consider it more difficult to implant the seeds: 50 cm^3 for ESTRO and 60 cm^3 for ABS. If otherwise suitable, these patients can be treated with hormones prior to the implantation in order to reduce the prostate volume. They make, moreover, recommendations regarding the type of brachytherapy: as monotherapy, as a boost after moderate dose external beam radiation or in conjunction with androgen deprivation.

Treatment planning: Both groups recommend that dosimetric planning of the implant be carried out for all patients before seeds insertion. The current standard of practice is to locate the volume using a TRUS in order to prepare the treatment plan containing needle location, number and strength of the seeds in each needle. TRUS is then used for guidance during the implantation procedure. Implantation before 1990s relied on distribution with even spacing of sources leading to a dose distribution with the central region of the implant receiving a higher dose. However, recent innovations in treatment planning systems and computer tomography have led to greater reliance on a more peripheral distribution of radionuclide loading method in

order to minimize the central hot spots. The reduction of the central dose is considered important because of the urinary complications with a higher urethral dose. Although urethral tolerance dose is not precisely known, doses in excess of 360 Gy with ^{125}I sources have shown significant complication rate (Wallner et al. 1996). So in the absence of better dosimetric data, the ABS recommends that modified peripheral method be used and that the urethral doses be carefully examined in an effort to minimize the length of urethra receiving more than 200% of the prescribed dose.

ABS and ESTRO recommend that postoperative dosimetry be performed for each patient in order to confirm the actual dose delivered or to identify any variance from the treatment plan. It also helps to assess the implant quality and is part of the learning curve. This procedure should preferably be done using CT images in order to demonstrate the relationship between the seeds and the prostate. Often the implantation of the seeds generates an oedema or bleeding that can affect the delimitation of the prostate on the CT scan. Therefore dosimetry based on CT scans performed too early could overestimate the size of the prostate. A delay of 4 to 6 weeks seems acceptable. The following recommended data should be reported:

1. The prescribed (intended) dose: the minimum peripheral dose to the margin of the target volume.
2. The D100: The dose that covers 100% of the prostate volume, which is the strict minimum peripheral dose. However, there is some uncertainty associated with delineation of the prostate on a CT scan. In the ESTRO recommendations this is replaced by the V150, the volume of the prostate that has received 50% more than the prescribed dose.
3. The D90: the dose that covers 90% of the volume to be treated. A D90 value greater than or equal to the prescribed dose is a measure of a good implant quality.
4. The V100: the percentage of the prostate volume that received the prescribed dose.

In the ESTRO recommendations, they also specify:

5. The volume implanted
6. The number of seeds
7. The number of needles used
8. the total activity implanted

If the dosimetry suggests significant underdosage in some portion of the prostate, the patient may be considered for additional external brachytherapy or a second implant as soon as reasonably feasible.

The dose prescribed for ^{103}Pd prostatic implant has been chosen lower than for ^{125}I implant (120 Gy against 145 Gy) mainly due to dose rate consideration (Chen and Nath 2003). The difference in half-live has for consequence that the time required to deliver 80% of the dose at full decay is roughly 3 times more for ^{125}I (140 days) than for ^{103}Pd (40 days). This difference in the dose rate can result in very different clinical response for a given total dose when the surviving cells in the irradiated tissue are

continuously proliferating and the sublethal damaged cells can be repaired during the process of dose delivery. Using a linear-quadratic model it was concluded that at clinically prescribed doses the predicted cell kill is better for ^{103}Pd in rapidly proliferating tumours, with an advantage for ^{125}I in slower-growing tumours.

b) Results:

Overall survival is a poor measure of treatment outcome for prostate cancer therapy because this is a slowly progressive disease that many men die with but not because of. There are many other medical conditions in elderly men that affect the death rate. Therefore, cause-specific survival based on death from cancer per se is a better measure. To evaluate a particular therapy and its efficiency in eradicating the disease, PSA disease-free survival is generally used in the case of prostate cancer. Because a rising in PSA post-treatment signals disease recurrence, it is an objective and early measure of disease status. Outcome is also very much dependent of prognostic factors such as tumour stage, histological grade (Gleason score) and pre-treatment PSA. Patients who have had prostatectomy can be additionally classified according to pathologic feature: extracapsular tumour extension, seminal vesicle involvement and lymph node status.

The results for surgery and radiotherapy, both external and brachytherapy are much the same. The best prognostic group, T1 to T2, PSA ≤ 10ng/ml, Gleason ≤ 6 has a PSA disease-free survival of 80% at 10 years both for radiotherapy and surgery. Similar patients show PSA disease-free status 80% to 90% of the time with implants. The implant patients tend to be a more highly selected group with smaller amounts of disease, which may account for the slightly better outcome statistics. Patients with more advanced disease, T3 or PSA greater than 10 ng/ml or Gleason 7 to 10, tend to have more guarded prognoses, once again, similar to those treated with surgery or radiation.

However, as radiation techniques become more highly conformal and doses are increased, early reports on outcome appear promising for the patients with more advanced disease.

c) Side effect and complications:

Surgery: With improved anaesthesia and surgical techniques and availability of antibiotics and other supportive care, operative mortality has been reduced to 1% or less. Other side effect can occur in very few patients like wound infection, haematoma or pelvic abscess (5%). Some problems may occur in 5% of the cases related to the removal of the lymph nodes. But the most significant morbidity is incontinence and sexual impotence, which is related to the type of radical prostatectomy. Moderate stress incontinence is reported to be 5% to 8% by major university centres. Surveys of patients, however, show this rate to be considerably higher at 25% to 30%. The

preservation of potency is related to the tumour stage, unilateral or bilateral resection of the neurovascular bundle and patient age.

Radiotherapy: Irradiation of the pelvic region may induce gastrointestinal side effect, with a higher incidence of both acute and late effects when larger volumes of the pelvis are irradiated. The incidence of severe gastrointestinal complications is low, 5%, with doses in the 64 to 70 Gy range, this rate more than doubles (14%) when higher doses of 75 to 81 Gy are applied. Sexual impotence has been observed in 30 to 60% of formerly potent patient with interstitial implants. These percentages are of course dependent on patient age, definition of potency and degree of potency pre-treatment.

Box 2: Staging system for carcinoma of the prostate tumours

Primary tumour (T)

TX Primary tumour cannot be assessed
T0 No evidence of primary tumour
T1 Clinically inapparent tumour neither palpable nor visible by imaging
T1a Tumour incidental histological finding in 5% or less of the tissue resected
T1b Tumour incidental histological finding in more than 5% of the tissue resected
T1c Tumour identified by needle biopsy (e.g. because of elevated PSA)
T2 Tumour confined with prostate
T2a Tumour involved one-half of one lobe or less
T2b Tumour involved more than one-half of one lobe but not both lobes
T2c Tumour involves both lobes
T3 Tumour extends through the prostate capsule
T3a Extracapsular extension (unilateral or bilateral)
T3b Tumour invades seminal vesicle(s)
T4 Tumour is fixed or invades adjacent structures other than seminal vesicles: bladder neck, external sphincter, rectum, levator muscles, and /or pelvic wall

Regional lymph nodes (N)

NX Regional lymph nodes were not assessed
N0 No regional lymph node metastasis
N1 Metastases in regional nodes(s)

Distant metastasis (M)

MX Distant metastasis cannot be assessed (not evaluated by any modality)
M0 No distant metastasis
M1 Distant metastasis
M1a Nonregional lymph node(s)
M1b Bone(s)
M1c Other site(s) with or without bone disease

Histologic grade

GX Grade cannot be assessed
G1 Well differentiated (Gleason 2-4)
G2 Moderately differentiated (Gleason 5-6)
G3-4 Poorly differentiated/undifferentiated (Gleason 7-10)

Stage grouping

I	T1a	N0	M0	G1
II	T1a	N0	M0	G2,3-4
	T1b	N0	M0	Any G
	T1c	N0	M0	Any G
	T1	N0	M0	Any G
	T2	N0	M0	Any G
III	T3	N0	M0	Any G
IV	T4	N0	M0	Any G
	Any T	N1	M0	Any G
	Any T	Any N	M1	Any G

2. Eye plaque treatment

An eye plaque is a mean of using radioisotopes with external application. Photon emitters like ^{125}I or ^{103}Pd and *b* emitters like ^{106}Ru/^{106}Rh are used in the management of uveal[§] melanoma of the eye, and more rarely retinoblastoma and haemangioma. Brachytherapy is employed in the management of this disease because of its ability to effectively treat tumours near the optic nerve and macula (see explanations box 3) without causing loss of vision secondary to radiation-induced changes in many cases. The sources are arranged in the plaque in appropriate positions so that adequate dose distributions are obtained (see Figure 5 and 6). The efficacy of the treatment method is often compared with stereotactic and proton therapy procedures, conformal modalities that strive to also deposit high doses of radiation to the tumour while sparing normal and sensitive tissues and structures.

Figure 5: Example of an ^{125}I plaque.

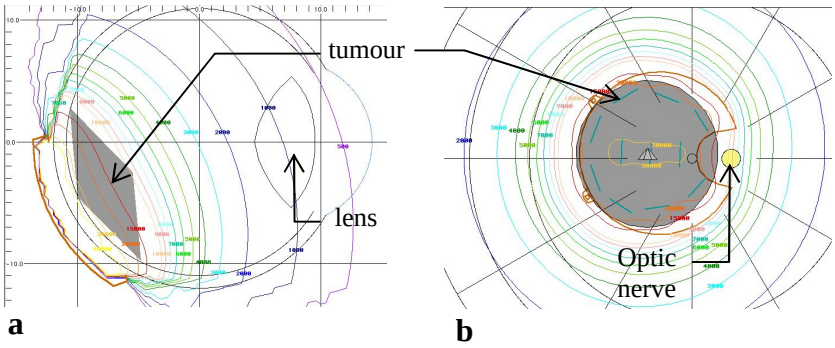

Figure 6: Example of an ^{125}I plaque and isodoses distribution calculated by the Bebig Plaque simulator treatment plan (Astrahan et al. 1990). Fig 6a is a 2D cut while Fig 6b. is the retinal diagram. The tumour is indicated in grey, the optical nerve in yellow.

Uveal melanoma is the most common primary intraocular malignancy in adults. It is almost invariably unilateral and has its highest incidence between the fifth and the seventh decades of age. It arises most frequently in the choroid (85%), less frequently in the ciliar body (9%) and in the iris (6%) (see Box 3). The tumour initially grows flat within the choroid, later it elevates Bruch's membrane and finally it ruptures through it

[§] The **Uvea** is the part of the eye consisting collectively of the iris, the choroid of the eye, and the ciliary body (see Box 3)

so that the melanoma assumes a characteristic mushroom-shape growing toward the vitreous humour. The retina over the surface of the tumour becomes elevated and detached (solid retinal detachment). This detachment gradually extends as a serious detachment over the slopes of the tumour. Uveal melanoma may precociously metastasize at distant sites including liver, lung, bone, kidney and brain in order of decreasing frequency. Extraocular orbital extension by contiguous spread also occurs if the lesion is left untreated. (see Table 1 for staging)

Box 3: Anatomy of the eye

1. Anterior chamber
2. Aqueous humour
3. Cornea
4. Iris
5. Lateral rectus muscle of the eyeball
6. Lens
7. Medial rectus muscle of the eyeball
8. Optic nerve
9. Posterior chamber
10. Retina
11. Vitreous body

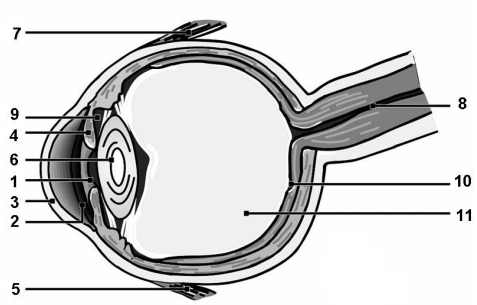

Figure B3: Schematic drawing of the eye anatomy

Definitions

- The **macula** is located roughly in the center of the retina, temporal to the optic nerve. It is a small and highly sensitive part of the retina responsible for detailed central vision.
- The **fovea** is the very center of the macula. The macula allows us to appreciate detail and perform tasks that require central vision such as reading.
- The **ciliary body** lies just behind the iris. Attached to the ciliary body are tiny fibers called zonules. The crystalline lens is suspended inside the eye by the zonular fibers. Nourishment for the ciliary body comes from blood vessels which also supply the iris. One function of the ciliary body is the production of aqueous humor, the clear fluid that fills the front of the eye. It also controls accommodation by changing the shape of the crystalline lens. When the ciliary body contracts, the zonules relax. This allows the lens to thicken, increasing the eye ability to focus up close. When looking at a distant object, the ciliary body relaxes, causing the zonules to contract. The lens becomes thinner, adjusting the eye focus for distance vision.

With age, everyone develops a condition known as presbyopia. This occurs as the ciliary body muscle and lens gradually lose elasticity, causing difficulty for reading.

- The **choroid** lies between the retina and **sclera**. It is composed of layers of blood vessels that nourish the back of the eye. The choroid connects with the ciliary body toward the front of the eye and is attached to the edges of the optic nerve at the back of the eye.

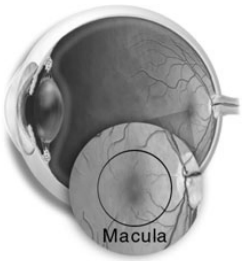

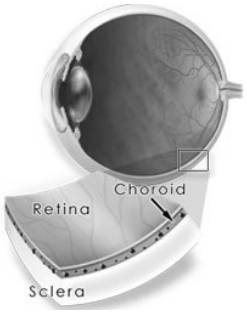

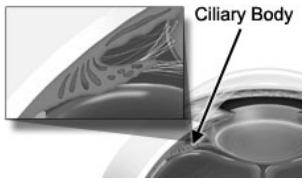

Uveal melanoma most often assumes a nodular or dome-shaped configuration, but occasionally tumours can be flat or diffuse and involve extensive areas of the uvea with little elevation.

Tumour size classifications according to boundary lines are as follows:

1. **Small**: Range from 1 mm to 3 mm in apical height and have a basal diameter of at least 5 mm.
2. **Medium**: Range from 2 mm to 3 mm up to 10 mm in apical height and have a basal diameter of less than 16 mm.
3. **Large**: Greater than 10 mm in apical height or have a basal diameter of at least 16 mm.
4. **Diffuse**: Horizontal, flat growth pattern, with the thickness of the tumour measuring approximately 20% or less than the greatest basal dimension; this uncommon variant of uveal melanoma seems to have a poorer prognosis.

Table 1: Staging of uveal melanoma.

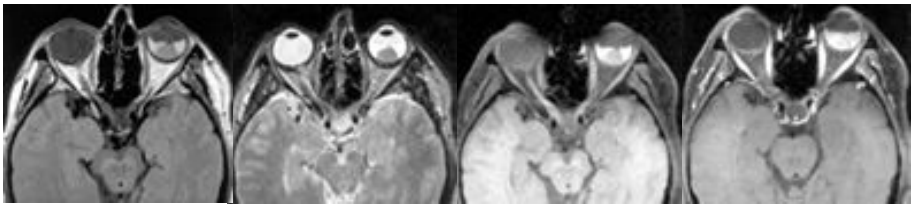

a **b** **c** **d**

Figure 7 a, b. MR, T1-weighted (a) and T2-weighted (b) images of the orbits. An isointense mass is seen in the left globe, growing toward the vitreous body. The mass is surrounded by a hyperintense retinal detachment. (c, d). Fat suppressed images, without (c) and with (d) contrast injection. The melanoma enhances following injection of contrast and becomes hyperintense (d).

a) Treatment techniques

For 100 years or longer, the usual treatment for choroidal melanoma has been removal of the eye, or enucleation. If the tumour has not spread to other parts of the body, then removal of the eye rids the patient of the tumour. According to the Collaborative Ocular Melanoma Study (COMS), enucleation is still the treatment of choice for large tumours or juxtapapillary tumour greater than 8 mm in apical height.

Since World War II, radiation treatment has also been used for choroidal melanoma. During the past 20 years, this method of treatment has been refined. Radiation, at the appropriate dose rates and in the proper physical forms, is intended to eliminate growing tumour cells without

causing damage to normal tissue sufficient to require removal of the eye. As the cells die, the tumour shrinks, but it usually does not disappear entirely. The two most commonly used forms of radiotherapy for local treatment are ophthalmic plaque brachytherapy and charged-particle (external beam) radiotherapy. Brachytherapy plaque treatment seems to be the most promising widely available method for irradiating medium choroidal melanoma (3.1 to 8 mm in thickness and no more than 16mm in the longest base diameter). Different types of radiation can be used: photons emitted by ^{60}Co, ^{125}I, ^{103}Pd or ^{198}Au, or betas emitted by ^{106}Ru. But satisfactory information about long-term results is still not available. The most used isotope is ^{125}I. The plaque treatment is considered as the treatment of choice by COMS for tumours no more than 20 mm in basal dimensions and no more than 10 mm in thickness.

High energy charged-particles (heavy ion or proton beam radiation) from a cyclotron also can be used to irradiate tumours. Surgery is performed first to sew small metal clips to the sclera so that the particle beam can be aimed accurately. Treatment is delivered over several successive days. The equipment needed for these treatments is available only in a few centres in the world. Good results have been reported in some patients, but many patients treated in this way have been followed for only a few years. Therefore, the long-term results of these forms of radiation therapy compared with the more commonly used plaque are presently unknown.

Over the years, other treatments have been used for a small number of patients. Photocoagulation using white light or laser light has been used to burn small tumours, and cryo-therapy has been used to kill the tumours by freezing them. These techniques are believed to work only for very small tumours. Some doctors have combined laser or cryotherapy with radiation, but such treatments are still experimental. A few patients have had eye wall resection[**] or a related procedure to remove tumours from their eyes. These methods of treatment are also considered experimental by most doctors and have been used only for a small number of tumours. No treatment is available that can guarantee to destroy the tumour, to preserve vision, or to assure a normal lifespan.

b) Results and consequences

(1) Enucleation

Enucleation surgery removes the tumour from the body if no spread outside the eye has occurred. Unfortunately, loss of vision for the eye removed is permanent because an entire eye cannot be transplanted. There is a reduced visual field on that side of the body when looking straight ahead and there is a loss of depth perception (stereopsis) as well. Many of the skills

[**] Removal of the portion of the eye that contains the tumour

of depth perception may be relearned with time. The cosmetic results after removal of the eye and fitting of an artificial eye are usually good. After enucleation there may be some temporary pain which can be relieved by medication. Possible surgical complications include haemorrhage, complications of anaesthesia, and late infection requiring removal of the implant. These serious problems are rare. Several years ago a suggestion was made that enucleation surgery might promote spread of tumour cells into the bloodstream during the operation and thereby lead to a reduced lifespan for the patient. This statement has never been proven and is not generally accepted as enucleation surgery for melanoma, like all cancer surgery, is performed in a way to minimize the possibility of spreading the cancer during the operation. Radioactive plaque therapy and eye wall resection also involve significant surgical manipulation of the eye. Thus, the risk of spreading the tumour by surgical manipulation is probably the same with enucleation as with other forms of therapy requiring surgery.

(2) Radiation treatments

The local control of radiation-treated uveal melanomas is dependent on radiation dose, dose rate, tumour location and length of follow-up – radiation effects are often delayed and so tend to increase with time of follow-up - and could be affected as well by intrinsic tumour-specific factors (e.g. cell type, melanin content, oxygenation and pH) that affect the radiosensitivity of the tumour. It can also be affected by the method of application. The influence of each factor is unfortunately very difficult to assess because of the lack of standardisation in the treatment delivery and in the definition of the target.

(a) Plaque treatment

When radioactive plaque therapy is successful, the tumour stops growing and may shrink over the course of 6 to 12 months. The patient keeps his or her own eye and, in favourable circumstances, when the tumour responds well and is located away from the most important parts of the eye, the tumour is destroyed and the patient may be able to see with the eye. This treatment is recommended by COMS, using ^{125}I, for medium tumours as enucleation does not offer a better chance of survival at 5 years (Robertson 2003).

Unfortunately, radiation from a radioactive plaque does not always destroy or inactivate the tumour. The tumour may grow and the eye may have to be removed at a later time. Delaying removal of the eye may allow the tumour to spread elsewhere in the body.

Radioactive plaque therapy requires two operations. Risks during surgery are similar to those described earlier for enucleation surgery. Compared to enucleation, there are added costs for a second operation, for the radioactive plaque, and for a longer hospital stay. Radiation almost

always damages some healthy parts of the eye. Radiation damage to the blood vessels of the retina (radiation retinopathy) or to the optic nerve often causes a gradual loss of vision. In some cases, haemorrhage into the inner part of the eye (vitreous cavity) may occur and causes loss of vision. Radiation damage to the lens may cause a cataract, which may require removal by surgery sometime later. Nearly one half of the patients treated with ^{125}I brachytherapy in the medium-size tumour arm of the COMS have lost substantial vision by three years.

After radioactive plaque treatment, many patients note some dryness and irritation of the eye which usually can be relieved by use of eye drops called artificial tears. In some instances, eyelashes may be permanently lost. In rare instances the outside layer of the eye (sclera) may become very thin. Occasionally, there may be prolonged redness, irritation, or infection inside the eye. The patient may see double if the muscles are damaged during the operation to apply or remove the plaque.

Relative Dose Distributions for Three Radiation Sources

	Iodine-125 Dose or [% of dose]	Palladium-103 Dose or [% of dose]	Ruthenium-106 Dose or [% of dose]
Posterior*			
Lens	14.00	9.00	0.00
Fovea	124.00	136.00	216.00
Optic nerve	103.00	106.00	140.00
Apex	8000 cGy	8000 cGy	8000 cGy
Base	384.00	463.00	946.00
Equatorial†			
Lens	25.00	18.80	0.04
Fovea	21.60	16.30	0.01
Optic nerve	19.80	14.10	0.01
Apex	8000 cGy	8000 cGy	8000 cGy
Base	384.00	463.00	946.00
Anterior‡			
Lens	59.00	55.00	15.00
Fovea	11.00	6.70	0.00
Optic Nerve	10.50	6.30	0.00
Apex	8000 cGy	8000 cGy	8000 cGy
Base	384.00	463.00	946.00

* 2 mm from the fovea and optic nerve.
† Centered at the equator.
‡ Centered at the ora serrata.
1 cGy = 1 rad. All 3 tumors are 10 × 10 mm (base) and 5 mm in height. All three tumors are centered at the vertical midline.

Table 2 : Relative doses at points of interest for the same absolute dose at the apex for three isotopes and three localisation of the tumour in the eye. (Finder 1997)

These side effects are very dependent on the dose received by the organs at risk. It may depend on the location and the size of the tumour, and on the type of isotope used. Table 2 shows typical doses at sensible points for a 5 mm thick tumour for 3 positions of the tumour and 3 isotopes. The prescription at the apex is always 80 Gy. The doses to other parts of the eye are dose relative to the prescription dose. For example, the dose to the fovea that can induce a loss of central vision vary drastically depending if the

tumour is located on the anterior part of the eye or on the posterior part. The use of beta particles seems also to be a benefit for organs at risk only if the tumour is located on the anterior or equatorial part of the eye. The very strong gradient obtained with betas must however be taken into account as it induces a dose as high as 946% of the prescribed dose, in this example, at the base of the tumour compared to 384% and 463% with ^{125}I and ^{103}Pd respectively (see Table 2). Those very high doses to the sclera, choroids and retina are more likely to cause secondary retinal detachment and relatively rapid chorioretinal scar formation with visual loss. (Finder 1997)

(b) High energy charged-particle therapy

The results obtained by this technique are also very good with a survival without metastasis at 5 years between 68% and 86% depending on the size of the tumour. The conservation of the vision is between 39% and 65%, depending equally on the tumour size (Noël et al. 2003). The complications that can occur following treatment with proton therapy depend on the dose given to the organs at risk, which are the optical nerve and the optical chiasma. When these doses stay below 60 Gy, the complications over 5 years are 3% and 4% respectively. The complications for lens, retina and parotid have been shown to be less than 5% for proton therapy and for IMRT (Mirabell et al. 2000). However, the results of the clinical trials are impaired by the low number of patients treated by this more expensive technique.

Studies report that the probability of eye retention after proton therapy is reduced when the height of the tumour is larger than 8 mm and the basal dimensions are larger than 16 mm (Munzenrider et al. 1988, Robertson 2003).

B. Physical context

1. Dosimetry

When looking at the clinical data, it is obvious that the choice between the techniques will be mainly related to the condition of the patient and the status of his tumour. Surgery, radiation therapy and other techniques are rarely in competition but rather each of these techniques is better adapted to one kind or stage of the disease, or to the general condition of the patient. When the choice has been made by the clinician for radiotherapy in general, and in our particular case, for brachytherapy, the physicist must consider how to administer the treatment so that the outcome for the patient will be as good as possible. This means that one must achieve a good local tumour control, often increased by a high dose to the tumour volume, and a good sparing of the organs at risk. In that context, the low photon emitters are candidates of choice for brachytherapy, allowing an escalation of the dose to the tumour while delivering minimal dose to the organs at risk.

In the clinical trials, it is clear that side effects and complications are often directly related to the dose that organs at risk have received during the treatment. It is then very important that the physicist be able to assess with a maximum of precision the dose delivered not only to the tumour, but also to the surrounding organs, sometimes at some distance from the seed implant. If it is not always possible to obtain the optimal sparing of tissues at risk, like in the case of the rectum in some configurations of prostate implant or of the optical nerve when the tumour is too close to it, a precise and accurate dosimetry could, at least, help to foresee which patients are more likely to suffer from side effects. These patients can be followed even more carefully.

However, the use of low energy photons induces some complications from the dosimetric point of view. Indeed, at these energies, the photoelectric effect begins to dominate, even in water. The attenuation is very high, so the penetration of these photons is quite short, which is of course an advantage for the patient, but it makes calibration and measurement quite difficult due to the high gradients. Moreover, the attenuation in the encapsulating metal is of course also very high, which makes the dosimetric characteristic around the seed very dependant of the internal design of the source. It is in fact so sensitive that some authors have pointed out the effect of the movement of the radioactive beads inside the seeds (Williamson 2002, Rivard 2001) or of the real thickness of the radioactive layer, although it is counted in microns (Karaiskos et al. 2001).

In the early stage of the clinical use of these isotopes, there was a high variability from investigator to investigator concerning basic data as the dose rate constant, the dose rate in water per unit source strength at 1cm along the perpendicular bisector of the source (cf. chap. II.C). The first reason for this situation was that some of the early dose rate constants were derived using a simple formalism for dose calculation suitable only for high

energy photon emitters like Radium. Secondly, the National Institute for Standard and Technology (NIST) has proposed a primary standard based on exposure only in 1985. Prior to that, the primary standard has been revised several times. The third reason for this variability was the large variety of phantom material used for the measurements: PMMA, liquid water or solid water. Due to the predominance of photoelectric effect, this had a large effect on the measurements. The experimental setups varied regarding the kind of used detectors — TLDs, ion chamber, photographic films, lithium-drifted silicon detector, and sodium iodine scintillator detector — or regarding the kind of phantom materials — PMMA, water equivalent plastic or even no phantom. All this lead to values for the dose rate constant for the ^{125}I seed model 6702 from Amersham from 1.03 rad cm^2 mCi^{-1} h^{-1} to 1.68 rad cm^2 mCi^{-1} h^{-1} (0.81 cGy cm^2 U^{-1} h^{-1} to 1.32 cGy cm^2 U^{-1} h^{-1})*.

This state has fortunately been improved during the years. First NIST has established a primary standard for Iodine seeds in 1985. Even if this standard has still been modified several times thereafter, this has certainly introduced a larger coherence between the studies. It was recognized too that correction factors were needed for measurements performed in materials other than water, for the dose rate constant as well as for the radial function (Luxton 1994, Meigooni et al. 1988) (see Chap II.C.).

Finally, in 1995, the report of the Task Group No. 43 (Nath et al. 1995) of the American Association of Physicists in Medicine has been published giving recommendation as to which data should be used in clinics for the available seeds. This report presents also a new formalism to be used for the analysis of the dose distributions around cylindrically symmetrical sources. It is presented in chapter II.C. Following this report, a vast number of studies have been published giving dosimetric data for new types of seeds, or comments about the formalism, sometimes with proposals for refinements for the formalism itself or for the measurements. This report unfortunately does not propose a standard for the determination of the dosimetric characteristics of the seeds. So in the studies that follow below, there is still a large diversity in the procedures used for the measurements of such dosimetric data, which are not always extremely well described.

The majority of the measurements are made with thermoluminescent detectors (TLD). Indeed, these detectors, as integrating detectors, are particularly well adapted for the usually low activity of the sources. They exist too in small sizes that allow the quite high spatial resolution needed for these studies. However, even within the studies using TLDs, differences exist that could affect the results if they are not properly addressed. The experimental setup can vary in many ways:

* The conversion factor used is 1.27 cGy cm^2 mCi^{-1} h^{-1}=1.00 cGy cm^2 U^{-1} h^{-1}, with U (cGycm^{2}h^{-1}) the unit for air kerma strength (Nath et al. 1995).

- The shape of the TLDs: rod (Wallace and Fan 1999, Wallace and Fan 1998, Wallace 2000, Duggan and Johnson 2001, Wallace 2002), chips (Chiu-Tsao and Anderson 1991), cubes (Nath et al. 2000, Chiu-Tsao et al. 2003, Patel et al. 2001, Anagnostopoulos et al. 2002, Nath and Yue 2001) mix of chips and cubes (Meigooni et al. 2000a, Popescu et al 2000, Meigooni et al. 2000b, Meigooni et al. 2002a, Meigooni et al. 2002b)
- For the chips, their positions relative to the seeds can be different: facing the seed such as in the studies of Chiu-Tsao (Chiu-Tsao et al 2003) or placed longitudinally like in the papers from Meigooni et al.(Meigooni et al. 2000a, Popescu et al 2000, Meigooni et al. 2000b, Meigooni et al. 2002a, Meigooni et al. 2002b).

However, other detectors have been used, such as diodes (Li et al. 2000a, Li et al. 2000b), mainly to measure directly in water, which TLD can not do. For these studies, generally the authors were able to obtain high activity sources from the company that manufactured them which counterbalanced the fact that the ratio signal/noise for diodes is quite bad when the dose rate is too low. Weaver (Weaver 1998) has used also a NaI scintillator for his measurement in air of the anisotropy function. Some tests have been performed with Gafchromic films (Chan and Prestwich 2002), but here too, the low sensitivity of those films was very limiting.

The materials used for measurements continue to be much diversified too: B-material mixture (Wallace and Fan 1998), Solid Water™ WT1 (Meigooni et al. 2000a, Popescu et al 2000, Meigooni et al. 2000b, Meigooni et al. 2002a, Meigooni et al. 2002b, Nath et al. 2000), RW1 (Wallace and Fan 1999), air (Weaver 1998), but the present common approach is to correct these measurements in order to obtain values in water using Monte Carlo simulations.

These Monte Carlo calculations are however again a source of discrepancies as there are many available Monte Carlo codes that can differ by their basic data or the approximations used in the physics. The following have been used for brachytherapy calculations. We give below a very brief description regarding the photon transport; a more complete description can be found in the literature.

- Integrated Tiger Series (ITS) (Halbleib and Mehlhorn 1983), expansions of the ETRAN code of Berger and Seltzer (1968). This code uses cross section data from Hubbell et al (1985). It takes into account relaxation and electron angular distribution (Sauter or Fischer) after photoelectric effect. Coherent scattering is calculated using atomic form factors from Hubbell and Øverbø (1979). Compton scattering is calculated with the Klein-Nishina equation corrected to take into account the electron binding effect but not the Doppler broadening effect. It has been used amongst others by Meigooni et al. (1988) and Nath et al. (1990).
- EGS4 (Nelson et al. 1985): uses the cross section data from Storm and Israel (1970). This code takes into account relaxation effect leading to

K_α and K_β after photoelectric effect, atomic form factors from Hubbell and Øverbø (1979) and uses the Klein-Nishina equation for Compton scattering. It has been used amongst others by Luxton et al. (Luxton 1994, Luxton and Joszef 1999), Wang and Sloboda (1996) and Weaver (1998).

- EGSnrc (Kawrakow 2000): uses the same cross section data from Storm and Israel (1970) as EGS4 but takes into account more physical processes than its predecessor. For the photoelectric effect, the interactions occur with single elements in mixtures and there is an optional angular electron distribution (Sauter 1931). The atomic relaxation is treated after creation of a vacancy. The same atomic form factors from Hubbell and Øverbø (1979) are used and there is a choice for Compton scattering between the use of the Klein-Nishina equation or of the Impulse Approximation approach (Ribberfors 1975, Ribberfors and Berggren 1982) to account for the interaction with bound electron and the Doppler effect.
- MCNP4 (Briesmeister 2000): also uses the cross section data from Storm and Israel (1967). For the photoelectric effect, fluorescent photons and Auger electrons are emitted after relaxation. The same atomic form factors from Hubbell and Øverbø (1979) are used for coherent scattering. For Compton scattering, the Klein-Nishina equation is used with corrections to take into account the interaction with bound electron and the Doppler effect. This code has been used for example by Wierzbicki et al (1998), Rivard (2001), Duggan and Johnson (2001), DeMarco et al. (2002) or Medich et al. (2003).
- MCPT (PTRAN) from Williamson (1988, Williamson et al. 1983). This code transports only photons and uses the cross section tabulated by Plechaty et al (1978) in the DLC-99 library. This library has been updated to the DLC-146 library in the later version. Many authors use this code as it is quite easy to use and as it is really dedicated to brachytherapy sources (Williamson 1988b, Meigooni et al. 2000a, Li et al. 2000a, Hedtjärn et al 2000, Popescu et al. 2000, Geareart et al. 2000, Kirov and Williamson 2001, Williamson 2002, Meigooni et al. 2002b, Patel et al. 2001, Daskalov and Williamson 2001, Li 2002, Chiu-Tsao et al. 2003).
- Home-made codes like the code described by Karaiskos et al. (2001) and Anagnostopoulos (2002).

All these codes differ slightly, for example by the different cross section libraries they use. Already in 1996 Wand and Sloboda (1996) had found that there could be differences in the results, depending on the cross section data used.

Some authors have also suggested that the geometry factor (see Chap. II.C) used in the TG-43 formalism could not be appropriate at short distances from the seed (Rivard 2001). For very short distances indeed, the exact distribution of activity inside the seed considerably influences the dose distribution. It is still an open discussion to decide if the geometry factor must reflect this physical reality or be considered as a mathematical tool

without real physical significance in close distance to the seed. This unfortunately brings differences in the radial function for short distances depending on the definition the authors choose for the geometry function.

All this leads to some discrepancies between the results published by different authors as can be seen on the graphs of Figures 8 and 9. For a same source, differences on the radial function calculated or measured by different authors can reach more than 10%.

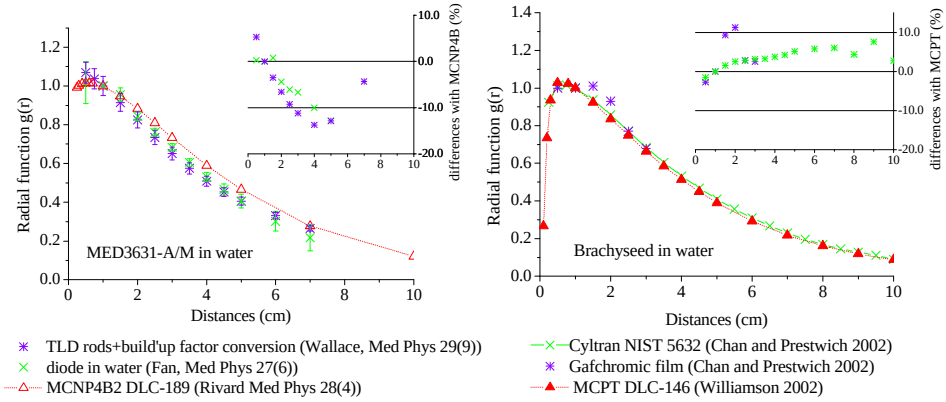

Figure 8: Radial functions calculated and measured by different authors and for different ^{103}Pd seeds.

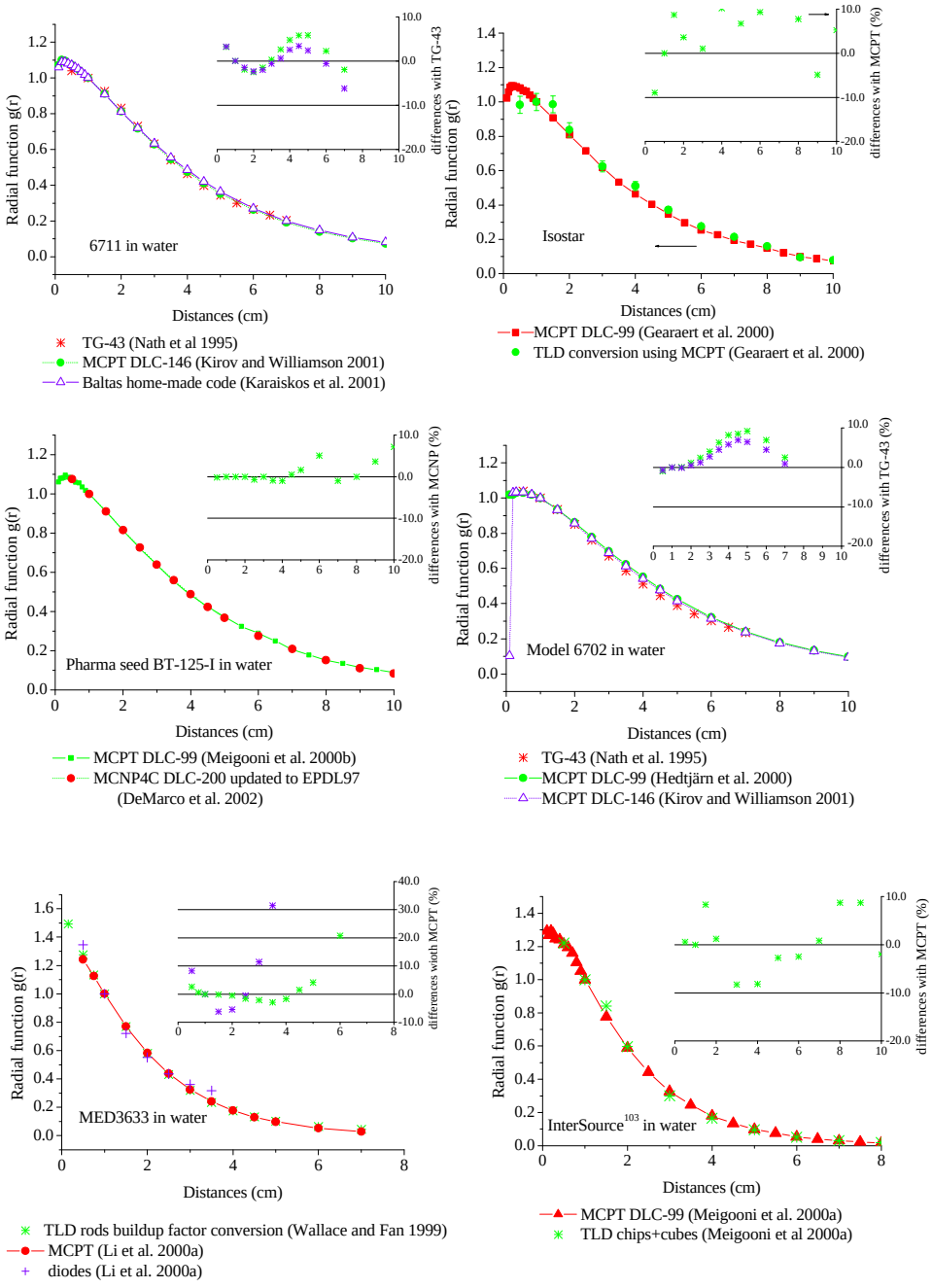

Figure 9: Radial functions calculated and measured by different authors and for different ^{125}I seeds.

Another problem has been discovered at the end of the 1990s concerning the calibration of these seeds. The outer shells of all these sources are made of titanium. The interaction of the photons emitted by ^{125}I or ^{103}Pd with the metal generates fluorescent photons of 4.5 and 4.9 keV. The presence of these low energy X-rays had already been pointed out by Kubo in 1985 (Kubo 1985). These extremely low energy photons are absorbed in the first millimetre of water, or of tissue and so they do not contribute to the dose delivered to the patient. However, the calibration is made in air, where these photons are much less attenuated, so they contributed to the kerma measured during the calibration process. In 1999, NIST has decided to remove the contribution of these low energy photons during the calibration by adding an Al filter in order to measure the activity related to the dose to the patient (see Box 4). This has reduced by 11% the Air Kerma strength measured on the ^{125}I seeds, and consequently the Dose Rate Constant of all the seeds that were already commercialised at the time had to be increased by the same amount in order to keep the same dose to the patient. For ^{103}Pd, this had no effect as the dose rate constant had not yet been determined. So the Dose Rate Constants of ^{103}Pd seeds were only measured with the new calibration. Concerning the calibration, another correction had to be made by NIST in 2000 because of a mistake in the procedure.

An overview of the data published for the dose rate constant for some seeds is shown in Table 3. The error for the experimental determination of dose rate constant is still high due to the combined uncertainty of the detecting methods (reproducibility of the TLD, positioning uncertainty…) to which must be added the problem of the sensitivity determination of the detectors to low energy photons. Monte Carlo calculations are not influenced by these, but other parameters can influence the results like the cross sections used (see example of model 6711) or the way the air kerma is calculated. Some authors have chosen a simplified method where they transport the photons in air and compute the air kerma at 1m. Others have chosen to model precisely the whole WAFAC calibration process (Williamson 2000) (see box 4). However, due to the high uncertainty of the measurements, it is still difficult to decide which method is the most relevant.

This confusing situation has very recently been recognised by AAPM that has published an update to the TG-43 (Rivard et al. 2004) containing new recommendations concerning the dosimetric data to be used in clinical applications based on the references used for Figures 8 and 9. This report is not yet complete; a second part must still be published, so it does not contain all the sources we are showing here. They also propose new recommendations concerning the information that must be reported in the studies about the determination of the dosimetric data around brachytherapy seeds in order to clarify the comparison between publications.

seed model	MC code	cross section library	material of measurements or calculations	detectors	dose rate constant in water ($cGyh^{-1}U^{-1}$)	references
6702					**1.039**	TG-43 (Nath et al. 1995)
6702	MCPT	DLC-99			**1.016**	Hedtjärn et al 2000
6702				TLD	**1.042**	Nath et al. 1990
6702				TLD	**1.076**	Chiu-Tsao et al 1990
6711					0.98	TG-43 (Nath et al. 1995)
6711	MCPT	DLC-146			**0.959**	Kirov and Williamson 2001
6711	home-made	plechaty			**0.953**	Karaiskos et al. 2001
6711	MCNP	updated			**0.957**	This work
6711	MCNP	DLC-200			**0.982**	This work
MED3631-A/M			RW1	TLD rods	**1.06**	Wallace and Fan 1999
MED3631-A/M			water	diode	**1.031/1.054**	Li et al. 2000b
MED3631-A/M	MCNP4B2	DLC-189			**1.067**	Rivard 2001
I25.S06	MCPT	DLC-99	water		**1.01**	Hedtjärn et al
I25.S06	MCPT	DLC146	water		**1.002**	Hedtjärn et al
I25.S06			RW1	TLD	**1.033**	Patel et al. 2001
Pharma seed BT-125-I			WT1	TLD cubes+chips	**0.90**	Popescu et al. 2000
Pharma seed BT-125-I	MCPT	DLC-99	water		**0.95**	Popescu et al. 2000
Pharma seed BT-125-I	MCPT	DLC-99	WT1		**0.92**	Popescu et al. 2000
Best mod 2301			WT1	TLD cubes+chips	**1.05**	Meigooni et al. 2000b
Best mod 2301	MCTP	DLC-99			**1.05**	Sowards and Meigooni 2002
Uroseed I125-SL S			PW2030	TLD	**0.95**	Wallace 2000
Uroseed I125-SL S	MCPT	DLC-99			**0.925**	Li 2002
3500 I-Plant			PW2030	TLD rod	**1.01**	Duggan and Johnson 2001
3500 I-Plant		DLC-189	PW2030	TLD rods	**1.01**	Wallace 2002
3500 I-Plant	MCNP	DLC-189			**1.017**	Rivard 2002

Table 3: Dose rate constants calculated or measured by different authors.

seed model	MC code	cross section library	material of measurements or calculations	detectors	dose rate constant in water ($cGyh^{-1}U^{-1}$)	references
Selectseed	home-made	plechaty			**0.954**	Karaiskos et al. 2001
Selectseed			solid water	TLD rods	**0.938**	Anagnostopoulos et al. 2002
InterSource			WT1	TLD	**1.02**	This work
InterSource	MCPT	DLC-99			**1.013**	Meigooni et al. 2002
InterSource				TLD cubes+chips	**1.013**	Meigooni et al. 2002
BrachyseedLS-1			WT1	TLD cube (alined)	**1.02**	Nath and Yue 2001
BrachyseedLS-1	MCPT	DLC-146			**0.935**	Williamson 2002
Echosees 6733			WT1	TLD cubes+chips	**0.99**	Meigooni et al. 2002

Table 3 (continued): Dose rate constants calculated or measured by different authors.

Box 4: WAFAC calibration

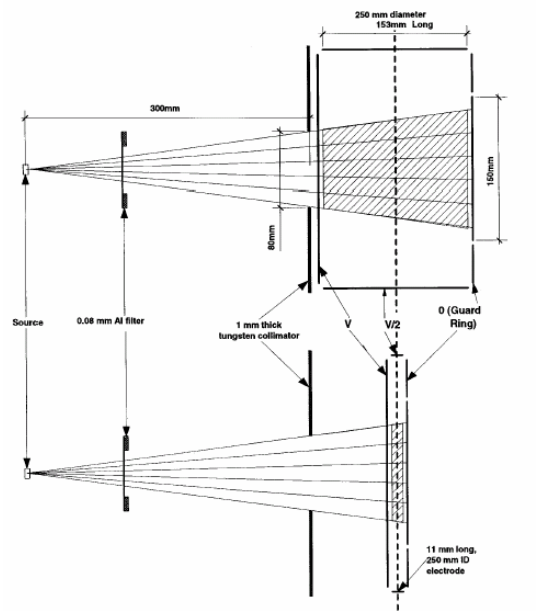

Figure B4: Side view of the wide-angle free-air chamber illustrating with the short 11 mm and the long 153 mm cylindrical electrodes in place. The chamber is cylindrically symmetric about the axis bisecting the seed centre, which is placed on a rotating holder during measurements to average over any equatorial anisotropy. The primary collimator located just upstream of the Al filter is not illustrated (Williamson 2000).

Since January 1999, the calibration of low energy photon seeds is made using the wide-angle free-air chamber (WAFAC) in National Institute for Standard and Technology (NIST) in Bethesda, Washington. The WAFAC is a cylindrically symmetric free-air chamber (see Figure B1) with circular electrodes on its proximal and distal faces consisting of very thin aluminised Mylar. The transverse axis of the seed to be calibrated is positioned on the WAFAC symmetry axis. WAFAC derives its name from the angular width of active volume (truncated cone of half-angle of 8° with respect to the source transverse axis), which is sufficiently large (715 cm^3) to allow calibration of single seeds. The middle electrode length can be varied so that wall scattering and electric field nonuniformities can be eliminated by subtracting the ionization current measured with the shorter electrode in place from that of the longer electrode applying:

$$S_{K,N99} = \frac{(I_{153} - I_{11})d^2}{r_{air}(V_{153} - V_{11})}(W/e)\prod_i k_i$$

where S_K is the air kerma strength of the source, I_t and V_t are net ionization current and active volume (aperture area multiplied by t), respectively, t is the electrode length (either 11 mm or 153 mm), d is the source-to-aperture distance, (W/e) is the average energy imparted to air per ion pair created (0.876 cGy/R), r_{air} is the density of air, k_i are various correction factors with values near unity, and "N99" subscript denotes traceability to the 1999 NIST standard. Finally, a thin Al absorber is used to remove low-energy Ti characteristic fluorescent X-rays photons from the beam.

2. Microdosimetry

The dose distribution is calculated for any treatment in order to optimise it for each patient or simply to report it correctly. The dosimetric part of this work is, however, fundamentally a macroscopic study. This means that it is implicitly assumed that matter is a continuous medium. In this context, it is possible to define the absorbed dose as the ratio between the energy deposited in a volume and the mass of that volume for the limit of an infinitesimally small volume. Unfortunately, the first assumption is not true. We know that matter is discrete, and so are the interactions between radiation and matter. To qualify the interactions between radiation and matter at a microscopic level, that discretisation cannot anymore be neglected. That same limitation exists for the quantity used classically to give the quality of a radiation: LET (Lineal Energy Transfer). This quantity is defined as dE/dx and measured in *keV/mm*. It describes the amount of localised energy transferred to the target per dx length.

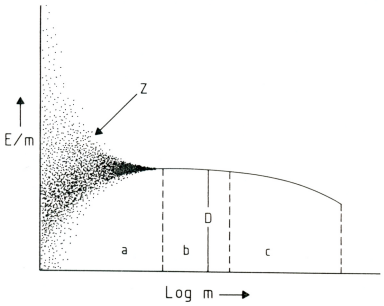

Figure 10: Variation of the dose (E/m) as a function of the mass m of the volume of interest (ICRU 36, 1983).

When the volume of interest is reduced, as shown in Figure 10, the dose begins to fluctuate, becoming more and more meaningless. Depending on the number and on the type of interactions occurring in the volume, the dose can vary wildly. The same happens with the concept of LET because those quantities are average quantities over large number of events. It is then no more possible to use these concepts at a very small level.

To deal with these fluctuations, a new branch of the dosimetry, called *microdosimetry* has been introduced by Rossi (Kellerer and Rossi 1972, Kellerer and Rossi 1978, Rossi 1959, Rossi 1960, Rossi 1967, Rossi 1968, ICRU 36 1983) who defined new concepts like the *specific energy z* or the *lineal energy y* that correspond to absorbed dose and LET respectively (see definition Chap II.B.). These quantities are stochastic. The specific energy is defined as the ratio of the energy imparted during a single energy deposition event in a volume to that volume and the lineal energy is defined as the ratio of the energy imparted during a single energy deposition event in a volume to the mean cord length of that volume. They are analysed in terms of distributions called *microdosimetric spectra* (MS) (ICRU 36 1983).

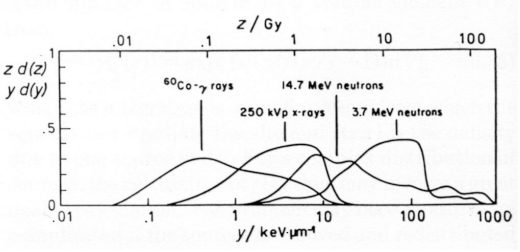

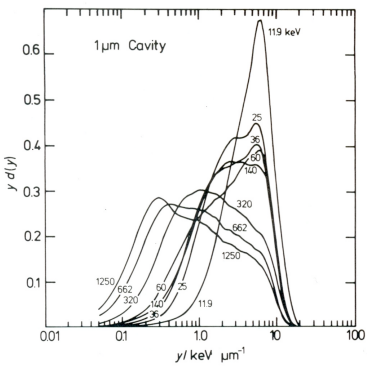

Figure 11: Examples of microdosimetric spectra for different types of radiations on the left and for photons of different energies on the right (ICRU 36 1983)

These distributions depend on the type of particles, as is shown in Figure 11. Particles known as low LET radiation, like photons, display distributions with a peak between 0.1 and 10 keV/µm. For high LET radiations, like neutrons, the peak is between 10 and several hundred of keV/µm, giving very different types of MS. The radiobiological effectiveness of these two types of particle is known to be very different, so there have been many attempts to quantitatively relate these microdosimetric parameters to the radiobiological effects.

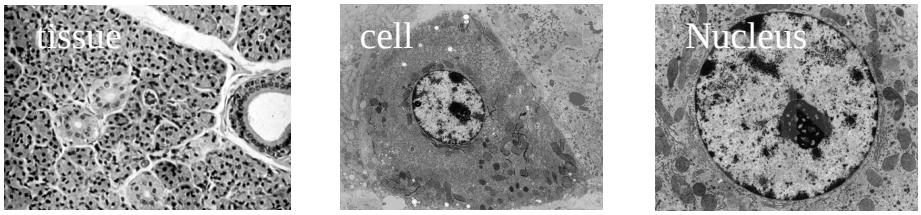

Figure 12: Histological sections of a tissue, a cell and nucleus.

However, this relationship is far from being trivial. In radiobiology, the interactions take place with living tissues. These are not inert continuous media; they are composed of living cells that possess themselves a complex internal structure (see Figure 12). It is known also that the different structures inside the cell are not equally sensitive to radiation. However, it is now clear that one of the most important components of this internal structure is the DNA located in the nucleus. DNA is the repository of hereditary information and the blueprint for operation of individual cells. Nearly all DNA damage is harmful. That is why the DNA is the only biomolecule that is specifically repaired thanks to redundancy in the contained information. All others are replaced. Unfortunately, this repair mechanism can have defects and limitations. It also introduces, from the point of view of our problem, a supplementary complication, as thanks to that repair mechanism, any hit is not lethal. So to have an idea of how

damaging an interaction will be in a living tissue, we need to know if the DNA is hit and if it is hit in a way that prevents repair. This does not take into account potential carcinogenic effects that radiation could induce.

This is a very complex task. One needs first to have a clear picture of the kind of damage a radiation can inflict to the DNA molecule. When photons interact with matter, they produce electrons that deposit their energy as ionisations and excitations of the atoms. These ionisations can generate damage to the DNA in the form of single-strand breaks (SSB) or double-strand breaks (DSB) (cf. Figure 13). These breaks can be caused by a direct interaction with the radiation, but also by free radicals produced by the radiation in water (cf. Box 5). In one or the other case, the damage is similar. These SSB can generally be repaired, but in the case of DSB where the two breaks are too close (for example at least less than 100 nm for V79 cells) to each other, the redundancy is lost and repair is not possible. Those lethal DSB are more likely to occur if the radiation deposits a large part of its energy over a small distance, i.e. when the density of ionization is high. In this case, clusters of ionizations appear that can be very harmful and damaging to the cells and by then they can harm the tissues in an irreversible way. This is the case for example for heavy ions that indeed have a very high radiobiological effectiveness (cf. Figure 14).

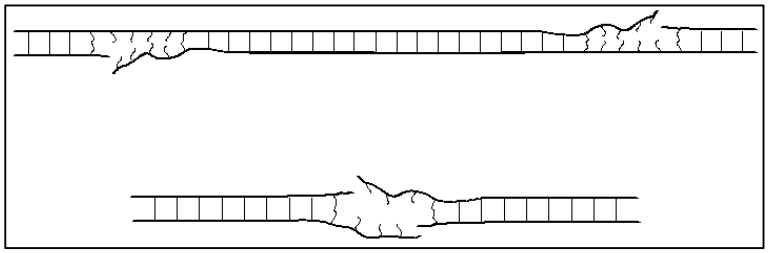

Figure 13: An idealized schematic comparing two single strand breaks (top) and one double strand break (bottom). A double strand break is formed when two or more strand breaks are formed in opposite strands of DNA within about 10 to 20 base pairs of each other. The lines between strands of DNA represent hydrogen bonds between complementary base pairs (Stewart 2001).

Box 5: Interaction of radiation with living tissues.

Direct and indirect actions

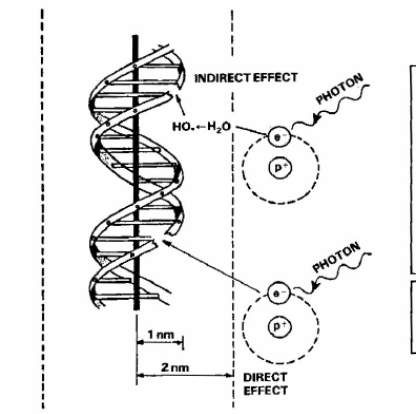

Radiolysis of water

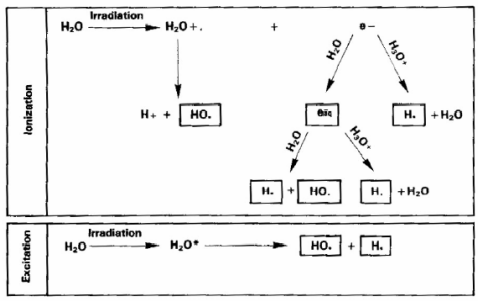

The effect of radiation on DNA can take two forms: direct or indirect (cf left figure).

- Direct : the interaction ionises an atom of the DNA molecule.
- Indirect: the interaction takes place with a water molecule which is ionized and the created free radicals such as HO• interact with the DNA.

The right diagram presents the kind of interactions that can occur with the water molecule to produce the free radicals.

The left part of Figure 14, for X-ray tracks, is an example of a particle with a low ionization density (low LET). The probability to create clusters of ionization that can generate DSB is low. On the contrary, in the right part, for a heavy-ion track, energy is deposited over a very short distance compared to the size of the DNA. The probability to destroy the DNA molecule is much higher.

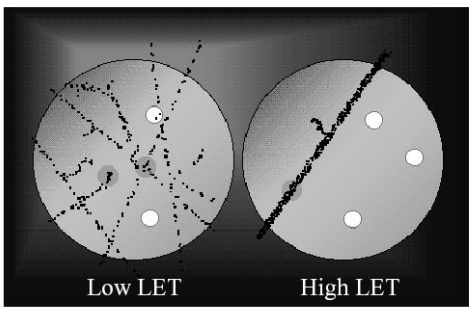

Figure 14: Comparison of the tracks of a low LET and a high LET particle.

The Relative Biological Effectiveness (RBE), defined as the ratio of the doses delivered with two different radiations causing the same effect in the same tissue, is used to quantify biologically the radiation quality. The study of Ling et al. (1995) has shown that ^{125}I has an RBE referred to ^{60}Co of about 1.4, meaning that for the same dose it is 1.4 times more

efficient at killing cells than ^{60}Co when it has been measured at 1.9 ± 0.7 for ^{103}Pd source (Ling et al. 1995). This is in agreement with the crude guess that can be made as the mean energy of ^{103}Pd is lower than the mean photon energy of ^{125}I and that consequently it deposits its energy over smaller distances, leading to a higher ionization density. The uncertainty on the RBE for ^{103}Pd, though, is very high and other studies about ^{125}I have given results between 1.2 and 2 (Scalliet and Wambersie 1987). The relative effectiveness of these isotopes is thus still far from settled. In the second part of this work, we have tried to analyse the physical aspects that can lead to a difference of biological efficiency between these two isotopes, relative to each other and relative to ^{60}Co.